

EE

19 JUL. 1988

HR/afm

CERN/PS/88-34 (AR)

**A Z-PINCH PLASMA LENS FOR FOCUSING HIGH-ENERGY PARTICLES
IN AN ACCELERATOR**

B. Autin, H. Gundel and H. Riege
CERN, Geneva, Switzerland

H. Bauer, E. Boggasch, J. Christiansen, K. Frank and R. Tkotz
Phys. Inst. University of Erlangen-Nürnberg, Erlangen, Fed. Rep. Germany

L. de Menna and G. Miano
University of Naples, Italy

F. Dothan
Hebrew University of Jerusalem, Israel

Abstract

The azimuthal magnetic field of a current-carrying plasma column, created in a z-pinch discharge, can be used to collect high-energy charged particles in accelerators. This powerful linear lens is superior to conventional focusing devices, owing to its high field gradient and lack of absorption. The plasma dynamics is studied with magnetic-field measurements, streak photography, and model computations. The results of the measurement and those of the long-term behaviour of a prototype lens designed for antiproton collection at the new CERN Antiproton Collector are presented.

Paper presented at the European Particle Accelerator Conference,
Rome, 7-11 June 1988

**PLEASE
MAKE A
PHOTOCOPY**
or check out as
**NORMAL
LOAN**

Geneva, Switzerland
June 1988

CERN LIBRARIES, GENEVA



CM-P00059144

A z-PINCH PLASMA LENS FOR FOCUSING HIGH-ENERGY PARTICLES IN AN ACCELERATOR

B. Autin, H. Gundel and H. Riege
CERN, Geneva, Switzerland

H. Bauer, E. Boggasch, J. Christiansen, K. Frank and R. Tkotz
Phys. Inst. University of Erlangen-Nürnberg, Erlangen, Fed. Rep. Germany

L. de Menna and G. Miano
University of Naples, Italy

F. Dothan
Hebrew University of Jerusalem, Israel

Abstract: The azimuthal magnetic field of a current-carrying plasma column, created in a z-pinch discharge, can be used to collect high-energy charged particles in accelerators. This powerful linear lens is superior to conventional focusing devices, owing to its high field gradient and lack of absorption. The plasma dynamics is studied with magnetic-field measurements, streak photography, and model computations. The results of the measurement and those of the long-term behaviour of a prototype lens designed for antiproton collection at the new CERN Antiproton Collector are presented.

1. Introduction

High-energy charged particle beams can be focused by magnetic quadrupole lenses, or by a device producing an azimuthal magnetic field B . Such a field can be created by a magnetic horn [1], or by a 'wire' [2] lens (Fig. 1). A wire lens is essentially a cylindrical conductor through which flows a strong axial current of uniform density. The resulting B -field, which is linearly increasing with radius inside the conductor, leads to simultaneous focusing in all transverse directions. A wire lens is the most efficient device for focusing antiprotons (\bar{p}) with a large production cone, as is the case for \bar{p} transferred to the new CERN Antiproton Collector (AC) ring. In the 'plasma lens' the conductor is a column of ionized gas. This gas is practically transparent for high-energy particles and does not deteriorate the emittance of the beam being focused. The plasma can carry much higher current densities than a solid conductor and can never be destroyed.

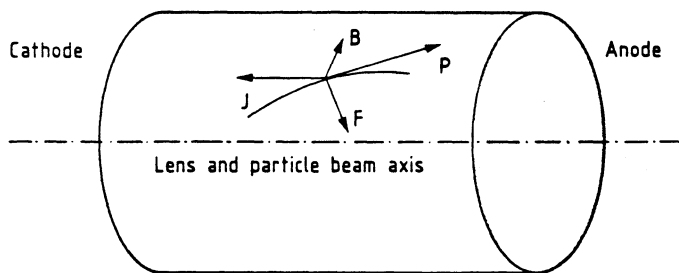


Fig. 1 Antiproton deflection inside a conducting column with current density j ; B , F , and p are the vectors of azimuthal magnetic field, force on and momentum of the particle.

The first plasma lens based on the z-pinch effect was designed, built, and installed in the Alternating Gradient Synchrotron at BNL in 1965 [3]. The upgrading of the CERN \bar{p} source requires a very powerful collector lens. A plasma lens with a plasma column of 40 mm diameter and 300 mm length carrying for $0.5 \mu\text{s}$ a current of 400 kA seems to be adequate. Such a lens can collect \bar{p} up to an angle of 0.2 rad emerging from an iridium target of 3 mm diameter and 55 mm length, situated 110 mm from the entry to the plasma column.

The current I_p needed to collect a beam of divergence α with a wire lens is given by

$$I_p = \frac{2\pi p}{\mu_0 e} \left(\frac{\alpha}{\sin \{ [(e/p)(\partial B/\partial r)]^{1/2} \cdot \ell \}} \right)^2, \quad (1)$$

where e is the elementary charge, p the particle momentum, $\partial B/\partial r$ the field gradient, and ℓ the length of the conductor [4]. Owing to the negligible absorption of a plasma one can make maximum use of the available length ℓ to approach $\pi/2$ for the argument of the sine function in Eq. (1) and hence reduce the current I_p to a minimum. The only restrictions come from the dimensions of the target and the construction of the lens.

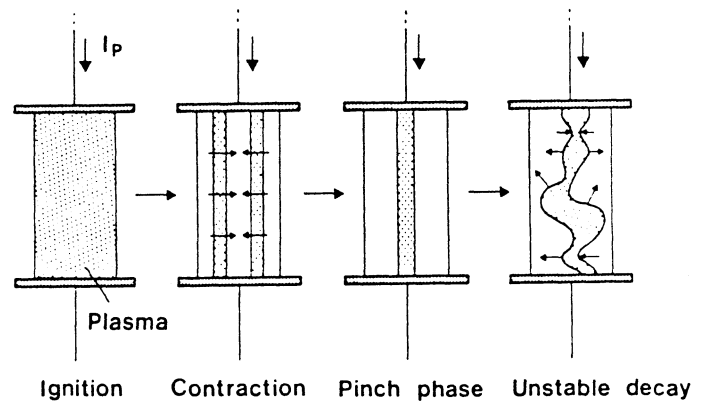


Fig. 2 Schematic representation of the plasma dynamics in a compression z-pinch induced by a current I_p .

In the plasma lens a pulse of high current flows through a partly pre-ionized gas, producing total ionization and an imploding plasma column (Fig. 2). The particles to be focused pass through the plasma lens shortly after the moment when the plasma column reaches its minimum ('pinch') diameter.

2. Experiments

For the use of a linear pinch in a particle accelerator, hollow electrodes are favourable [4, 5]. Such a structure needs only thin windows in the rear electrode walls for the passage of the beam. The z-pinch tube is filled with hydrogen, helium, or argon at pressures ranging from 10 to 1000 Pa. It is inserted symmetrically into a strip-line table which is linked to four capacitor banks of 108 μF total capacitance [6]. Each capacitor bank is linked to the central strip-line table by a sandwich strip-line containing a high-current pseudospark switch. Charging voltages V_0 of up to 20 kV were applied.

Two Rogowski-type current pick-up loops for total current measurement [7] are wound around the plasma tube. The voltage between the plasma-tube electrodes is measured with commercial high-voltage probes. The magnetic field and current distributions

inside the tube are determined as a function of time by two minute electrically screened coils [4, 5]. The coils can be moved in the radial direction. The spatial and temporal stability of the plasma column in the z-pinch tube was studied with streak photography using horizontal and vertical slits (Fig. 3). Simultaneous magnetic field

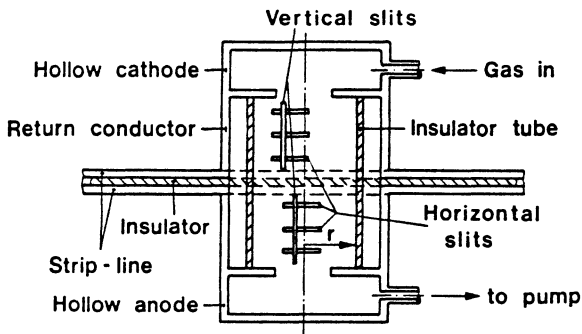


Fig. 3 Positions of the vertical and horizontal slits for streak measurements of the plasma dynamics in the plasma lens.

measurements not only enabled the field distribution to be determined in one longitudinal position, but also allowed it to be extrapolated over the whole length of the tube.

Figure 4 shows a representative oscillogram of magnetic field, pinch current, and pinch voltage for a capacitor bank voltage (V_0) of

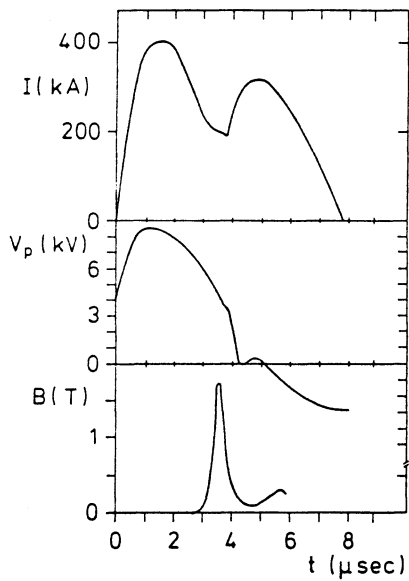
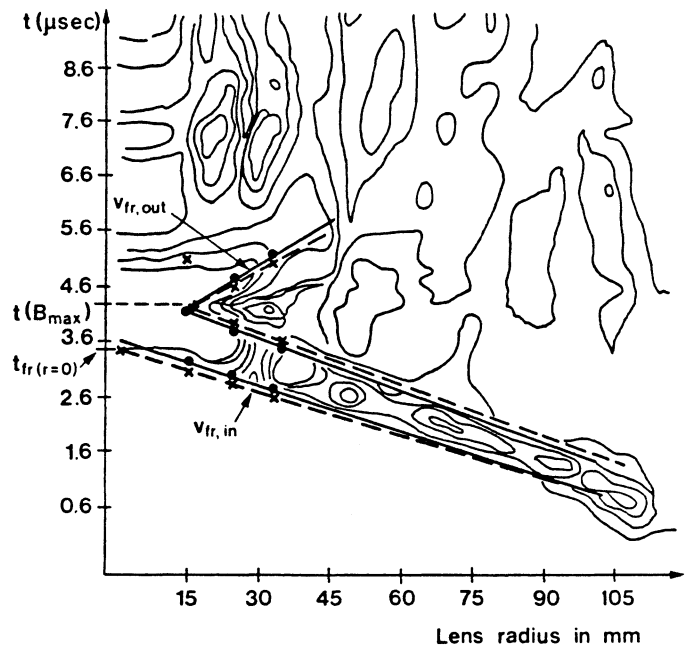


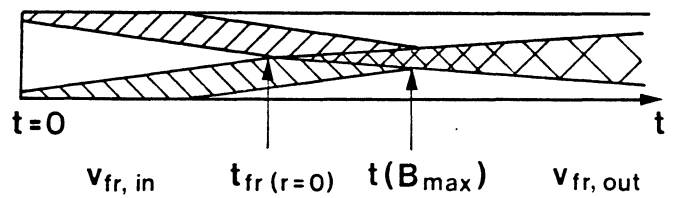
Fig. 4 Total current I , pinch voltage V_p , and azimuthal magnetic field B (at radius 10 mm) as a function of time; 400 Pa of hydrogen in an alumina tube; $V_0 = 15$ kV.

15 kV and a hydrogen fill of 400 Pa. Figure 5a shows results of measurements of current density j as a function of time and radius, for a hydrogen fill of 400 Pa and a charging voltage of 15 kV. The imploding current layer can also be observed by streak photography. Figure 5b shows a streak picture, which gives the same result for the implosion rate as the magnetic measurement, and which defines the significant time values of the pinch process.

Figure 6 shows the 'inverse skin effect' (IS) [5, 8, 9] that occurs in any conductor when the skin depth becomes comparable with the conductor radius. It is characterized by induced current loops



a)



b)

Fig. 5 Comparison of light emission from the z-pinch plasma measured by streak photography (dashed lines = cathode side and full lines = anode side) with current density j (isolines) as a function of radius and time (a). The corresponding horizontal streak picture (b) shows the significant moments of the contraction and expansion phase; 400 Pa of hydrogen in a quartz tube, $V_0 = 15$ kV.

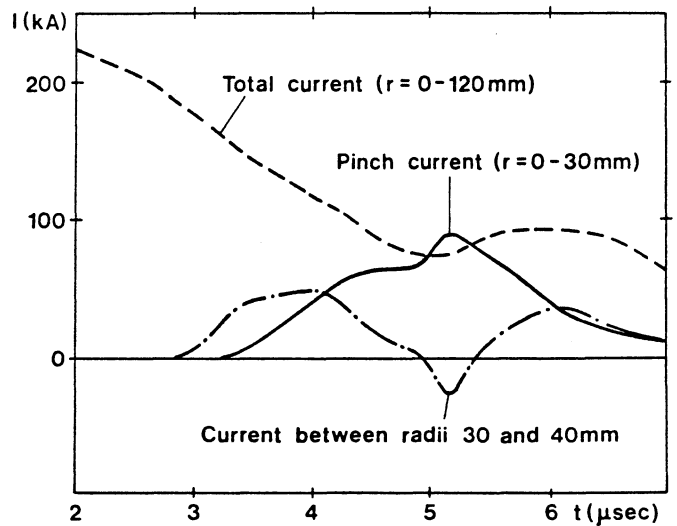


Fig. 6 Total current, pinch current, and current between 30 and 45 mm radius for 600 Pa of hydrogen in a quartz tube, $V_0 = 15$ kV. Note the pinch enhancement and negative-current shell induced by the 'inverse skin effect'.

('inductons'), which amplify the internal (pinch) current and excite negative current shells at the outer surface that are rapidly ejected outwards. An approximate description of the IS is given by

$$\dot{I}_p [(1/2) + \ln(r_a/r_p)] < I_p \dot{r}_p / r_p, \quad (2)$$

where I_p is the pinch current, r_p the pinch radius, and $r_a > r_p$. For a solid conductor only $\dot{I} < 0$ generates the IS. In an expanding plasma column ($\dot{r} > 0$) condition (2) can also be fulfilled for $\dot{I} > 0$, especially at high I_p and small pinch radius. In this case IS has a stabilizing effect on the plasma column!

3. Model computations and comparison with experimental results

In order to operate a future plasma lens at the AC target the development of a theoretical model is necessary. Earlier models, such as the 'snow-plough' model [10], the 'snow-plough energy' model [11], or the slug model [12] failed to describe real z-pinchs of our type. The approximations of a fully ionized plasma with infinite conductivity and the formation of an infinitely thin, imploding current sheet lead to strong deviations from experiments. In reality, the gas is only weakly ionized at the start. The substantial energy expenditure to dissociate the gas (e.g. when using hydrogen) and to ionize it cannot be neglected and must appear in the energy-balance

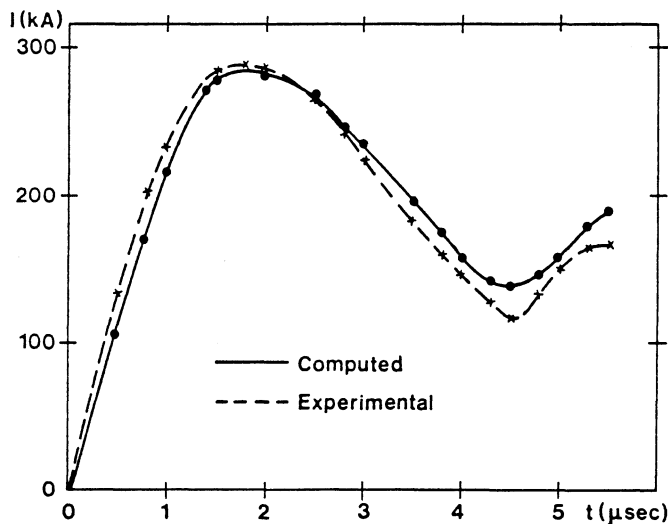


Fig. 7 Comparison of measured and computed total current for hydrogen at 400 Pa in a quartz tube and $V_0 = 10$ kV.

equation. A model including shock waves, initial ohmic resistance, ionization and dissociation energy losses, and a degree of ionization below 100%, has been developed and successfully compared with the latest prototype measurements. A particular comparison for hydrogen in an Al_2O_3 tube is shown in Fig. 7. Wall currents and inductons induced by IS are not yet included in this model.

4. Long-term behaviour

Since the AC plasma lens has to be pulsed every 2.4 s for at least 1.5 million pulses without interruption, the measurements of the deterioration of electrodes and insulator tubes are essential.

Evaporation rates of different insulator materials were determined by the measurement of weight loss or the increase of the internal diameter of the tube. Erosion rates can best be estimated from the geometrical change of the electrode shape. The insulator wall materials which evaporate induce strong wall currents and vice versa. The wall currents in silica start earlier and are at least twice as strong as those in an Al_2O_3 tube. The eroded wall material is mainly deposited on the cool electrodes and beam windows, leading to a change in performance and eventual failure of the plasma lens. Here some erosion rates obtained in life tests at 16 kV charging voltage are quoted:

Quartz/argon	35 Pa	7.5 mg per pulse
Alumina/argon	35 Pa	3.2-4.7 mg per pulse
Boron nitride/hydrogen	400 Pa	1 mg per pulse
Alumina/hydrogen	400 Pa	< 0.1 mg per pulse

Electrode erosion rates are at least one order of magnitude smaller than the best insulator erosion rates. With the last combination and tungsten electrodes a lifetime far beyond 10^6 pulses can be assumed.

5. Outlook

A wide parameter range has been covered with the experiments on plasma lens prototypes described in this paper. Scaling from the experimental and numerical results shows that for the final AC plasma lens a new pulse generator is required, featuring a cycle time of more than 30 μ s (twice that of the present test generator) and a stored pulse energy of 20 kJ at 20 kV charging voltage. The final alumina lens tube will have a length of 270 mm and an internal diameter of 200 mm. The filling gas will be hydrogen. Under these conditions the design specifications for the plasma column radius, for the magnetic-field amplitude, and for the field duration can be met. The entrance and exit windows of the plasma lens are left as an open problem until beam tests can be performed in the AC target area.

References

- [1] S. van der Meer, CERN 61-7 (1961).
- [2] B.B. Bayanov et al., Proc. Xth Int. Conf. on High-Energy Accelerators, Protvino, 1977, Vol. II, pp. 103-109. Translated by AD-EX Translations International, USA (1984).
- [3] E.B. Forsyth, L.M. Lederman and J. Sunderland, IEEE Trans. Nucl. Sci. NS-12 (1965) 872.
- [4] B. Autin et al., IEEE Trans. Plasma Science, PS-15, No. 2 (1987) 226. (Special Issue on Plasma-Based High-Energy Accelerators.)
- [5] F. Dothan et al., J. Appl. Phys. 62 (9) (1987) 3585.
- [6] E. Boggasch, V. Brückner and H. Riege, Proc. 5th IEEE Pulsed Power Conf., Arlington, Va., 1985 (85C 2121-2 of IEEE Catalog, New York, 1985), p. 820.
- [7] E. Boggasch and R. Grüb, Internal report CERN/PS/86-25 (AA) (1986).
- [8] M.G. Haines, Proc. Phys. Soc. 74 (1959) 576.
- [9] E. Boggasch, Dr. Arbeit, Univ. Erlangen-Nürnberg (1987).
- [10] M. Rosenbluth, H. Garwin and A. Rosenbluth, Infinite Conductivity Theory of the Pinch, Los Alamos Scientific Lab. Rep. LA-1850 (1954).
- [11] T. Miyamoto, Analysis of high-density z-pinchs by a snow-plough energy equation, Nucl. Fusion 3 (1984) 337.
- [12] D. Potter, The formation of high-density z-pinchs, Nucl. Fusion 18 (6) (1978) 813.